Publications

Available Online

J. Sci. Res. **16** (3), 803-815 (2024)

JOURNAL OF SCIENTIFIC RESEARCH

www.banglajol.info/index.php/JSR

Synthesis and Characterization of Carboxymethyl Cellulose/Poly(Acrylamide-co-Vinyl Imidazole) Based Self-healing and pH-sensitive Hydrogel (Part-I)

D. Dubey*, S. K. Bajpai, M. Bajpai

Polymer Research Laboratory, Department of Chemistry, Govt. Model Science College, Jabalpur (M.P.)-482001, India

Received 18 November 2023, accepted in final revised form 13 January 2024

Abstract

In the present work, monomers acrylamide (AAm) and vinyl imidazole (VI) were co-polymerized in the presence of carboxymethyl cellulose (CMC) to yield a totally un-crosslinked solid hydrogel electrolyte (SHE) with fair self-healing property. The SHE was characterized by FTIR, XRD, SEM, and TGA analysis. The surface texture, as revealed by SEM analysis, was observed to be fairly smooth. The hydrogel electrolyte exhibited pH-dependent swelling behavior with percent equilibrium swelling (PES) of 5170, 1892, and 5163 in the swelling media of pH 1.0, 6.8, and 13.0, respectively. In addition, the kinetic swelling was best interpreted by the Power function model, revealing a chain relaxation-controlled water uptake at pH 1.0 and 13.0. The SHE showed an excellent self-healing property, which was confirmed by the "LED glowing" experiment. As compared to its original elongation of 200 %, the self-healed hydrogel exhibited an elongation of 157 %, thus showing a fair restoration tendency.

Keywords: Solid hydrogel electrolyte; Uncrosslinked hydrogel; Self-healing; pH-dependent swelling; Hydrogen bonding; Kinetic models.

doi: https://dx.doi.org/10.3329/jsr.v16i3.69941 J. Sci. Res. **16** (3), 803-815 (2024)

1. Introduction

In the last few years, hydrogels with self-healing properties have been a focus of attention for material scientists, probably due to a wide range of their applications in different fields like wearable, flexible devices, [1-3] electronic skin, [4,5] biomedicine, [6-8] tissue engineering, [9,10] cell therapy, wound dressing, [11,12], etc. A number of approaches have been employed to fabricate self-healing hydrogels. These include hydrogen bonding interactions, host-guest recognition, electrostatic interactions, hydrophobic associations, metal-ligand coordination, dynamic covalent bond formation, etc. [13-18].

A fairly high water content, flexibility, and adhesiveness are the basic requirements for the use of these hydrogels in biomedical fields such as tissue engineering. On the other hand, using these hydrogels as storage energy devices requires high conductivity, flexibility, and fair mechanical strength. However, the development of a hydrogel with all

* *Corresponding author*: sunil.mnlbpi@gmail.com

the properties mentioned above still remains a challenge. The reason is that fairly high water content usually results in a brittle polymer matrix. On the other hand, a fairly high movement of polymeric segments is required for self-healing property, but this automatically reduces the mechanical strength. [19,20] Therefore, in order to have a hydrogel with all such desired properties, a proper selection of monomers and polymers is required so that the polymer, formed, has an appropriate combination of hydrophilicity, bonding strength, presence of protonated /deprotonated groups and mutual entanglements of polymer chains.

In the present work, a sincere attempt has been made to fabricate a physically crosslinked hydrogel with electrical conductivity, self-healing, anti-freezing, and adhesiveness. The solid hydrogel electrolyte (SHE) has been synthesized using a polysaccharide carboxymethyl cellulose (CMC) and a copolymer poly (acrylamide-co-vinyl imidazole (AAm-co-VI). The rationale for the selection of these constituents is as follow: (i) CMC is a highly water-soluble polymer with hydrophilic groups that have fair tendency to interact with water molecules, (ii) the copolymer poly(AAm-co-VI) contains amide and imidazole groups respectively, that can produce intermolecular H-bonding interactions to provide a stable polymer matrix with proper water holding capacity and fair tendency of self-healing, and (iii) mutual entanglements between CMC polymeric chains and linear copolymer poly (AAm-co-VI) segments provide additional stability to the polymer matrix.

In this way, the proposed solid hydrogel electrolyte (SHE) system has excellent self-healing and adhesive properties with fair flexibility and electrical conductivity. In addition, the presence of ionizable moieties provides a conducting property to the gel that can be further enhanced by the addition of electrolytes during the preparation of SHE. To the best of our knowledge, a hydrogel system consisting of CMC and copolymer poly (AAm-co-VI) and having H-bonding interactions as a physical crosslinker has not been reported to date.

2. Experimental

2.1. *Materials*

The monomer Acrylamide (AAm) and Vinyl imidazole (VI) were obtained from Hi-Media Chemicals, Mumbai, India. The inhibitor, present in acrylamide, was removed by distillation with methanol. Carboxymethyl cellulose (CMC), initiator potassium persulfate (KPS), and other salts were also purchased from Hi Media Chemicals and were analytical grade. All the experiments were performed using distilled water.

2.2. *Preparation of solid hydrogel electrolyte (SHE)*

The SHE was prepared by carrying out free radical co-polymerization of monomers AAm and VI in the presence of dissolved CMC. The pre-determined quantities of monomers AAm and VI were mixed into a definite volume of CMC solution, followed by the addition of glycerol (if required) and initiator KPS. The pre-polymerization mixture was poured into

plastic rectangular molds and kept in an electric oven (Tempstar, India) at 40 ºC for 1 h. Finally, the films were taken out carefully and placed in Polyethylene bags for further use. In all, four samples with different compositions were prepared, as given in Table 1.

Table 1. Composition of various solid hydrogel electrolyte samples prepared.

Sample code	Composition of SHE samples*			
	CMC (g)	AAm (g)	VI (mL)	Glycerol (mL)
SHE-I	0.64	6.0	3.0	-
SHE-II	0.64	6.0	3.0	2.0
SHE-III	0.64	6.0	3.0	3.0
SHE-IV	0.64	6.0	3.0	4.0

2.3. *Characterization of the SHE*

The Fourier Transform Infrared (FTIR) spectra were recorded with an FTIR spectrophotometer (Shimadzu, 8400, Japan) using KBr. The powdered sample was mixed with KBr. The scans recorded were an average of 100 scans, and the selected spectral range was between 400 to 4000 cm^{-1}.

The X-ray diffraction (XRD) method was used to determine the crystalline nature of hydrogels. These measurements were carried out on a Rikagu Diffractometer (Cu radiation = 0.1546 nm) running at 40 kV and 40 mA. The diffractogram was recorded in the range of 2θ from 3 to 80° at the speed rate of 2 degrees/min.

2.4. *Measurement of water absorption behavior*

A pre-weighed piece of the sample SHE-I was placed in 250 mL of the swelling medium of definite pH and its mass measurements were made at definite time intervals till the attainment of equilibrium. The percent swelling (PS) was calculated using the following expression:

$$PS = \frac{W_t - W_o}{W_o} \times 100 \quad (1)$$

Where, Wo is the initial dry mass, and W_t is the mass of the sample in the swollen state at time 't'.

In order to study the effect of the pH of the swelling media on the water absorption behavior of hydrogels, buffer solutions of different pH were prepared, and the pre-weighed pieces of sample SHE-I were equilibrated for a period of 48 h to allow the samples to attain equilibrium swelling.

2.5. *Self-healing studies*

2.5.1. *"LED glow experiment"*

Two terminals of a 5-volt battery were connected to an LED bulb, and a strip of hydrogel sample SHE-I was also introduced in the electric circuit. The LED bulb started to glow.

Now, the hydrogel was cut into two parts using a sharp blade. Due to a break in the electrical circuit, the LED bulb blew off. The cut pieces of the hydrogel sample were brought into contact for five minutes. As a result of the healing of the gel, the LED bulb started to glow again.

2.5.2. *Gel stretching experiment*

A piece of hydrogel sample SHE-I of definite length was stretched and then brought back to its original length. Now, the hydrogel was cut into two pieces, and the cut ends were put in contact for self-healing. After the gel was healed, it was again stretched, and the percentage of elongation was measured.

2.5.3. *Construction of geometries/letters*

A long piece of hydrogel sample SHE-I, in the form of a thick fiber, was cut into pieces, and the cut ends were brought into contact for a definite time period to make different geometrical shapes.

3. Results and Discussion

3.1. *Preparation of SHE*

In this work, solid hydrogel electrolyte (SHE) was prepared by carrying out free radical-initiated polymerization of monomers AAm and VI in the presence of dissolved CMC in aqueous medium. As no crosslinker has been used in the reaction mixture, the linear chains of copolymer poly (AAm-co-VI) and carboxymethyl cellulose (CMC) were entangled with each other to form a closed matrix. The matrix, thus formed, was additionally stabilized due to hydrogen bonding interactions between carboxymethyl groups of CMC, imidazole groups of VI, and amide group of AAm. In fact, these H-bonding interactions play a major role in empowering SHE with self–healing and adhesion properties. All such possible H-bonding interactions are illustrated in Fig. 1.

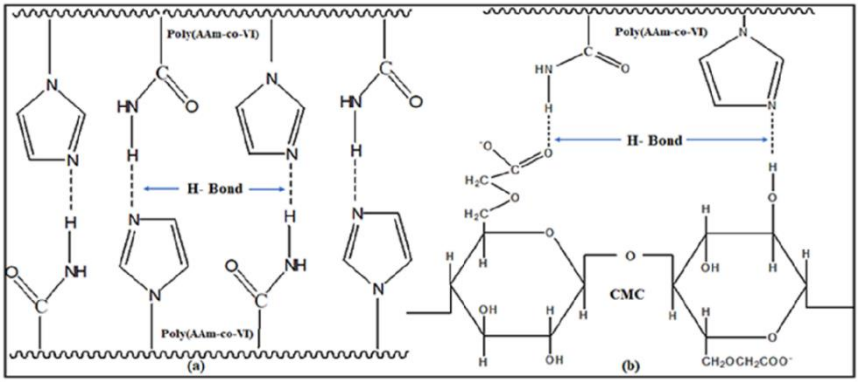

Fig. 1. Possible H-bonding interactions within the hydrogel matrix.

3.2. *Characterization*

3.2.1. *Fourier transform infrared spectroscopy analysis (FTIR)* –

The FTIR spectrum of sample SHE-1, composed of CMC and Poly (AAM-co-VI), is shown in Figs. 2a-b. The spectrum contains nearly all the characteristic peaks of its constituents. The characteristic transmission band at 3040 cm^{-1} shows the hydrogen bonding OH stretching region, and a peak observed at 1602 cm^{-1} confirms the presence of COO^- (carboxyl group). This band was important in determining the hydrogen bonding between CMC and AAm-co-VI. The small hump at 2928 cm^{-1} and 2850 cm^{-1} may be assigned to C-H stretching in the copolymer chain. The absorption band at 3330 and 3490 cm^{-1} shows the intermolecular hydrogen bonding NH_2 stretching vibration region. [21,22]. The absorption bands at 1497 and 1544 cm^{-1} are attributed to the N–C and C–C stretching vibration of the VI chain. The bands at 760 and 660 cm^{-1} show C–H ring bending vibration and C–N vibration of the azole ring, respectively. [23,24]. The band at 1060 cm^{-1} is due to the CH-O-CH_2 stretching of CMC [25].

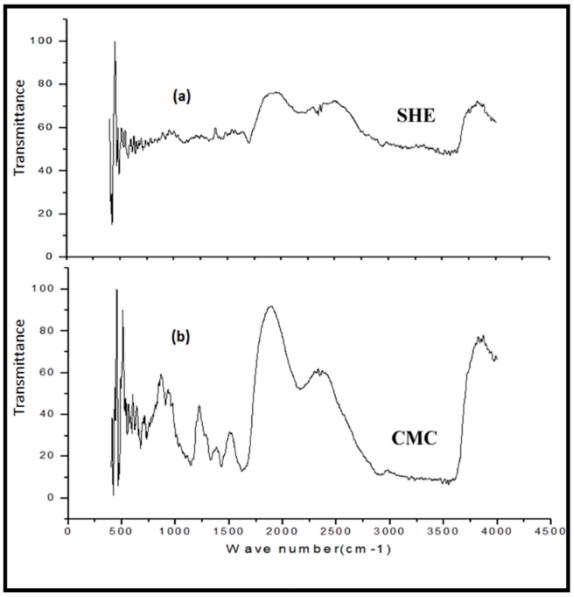

Fig. 2. FTIR spectrum of (a) CMC and (b) sample SHE-I.

3.2.2. *Scanning electron microscopy analysis (SEM)*

The surface texture of the film sample SHE-I was investigated by SEM analysis. The SEM images shown in Figs. 3a-c were obtained with 3000, 10000, and 30000 X magnifications. In all the images, no agglomerations, cracks, voids, or any other defect was observed. The film surface was very smooth and even.

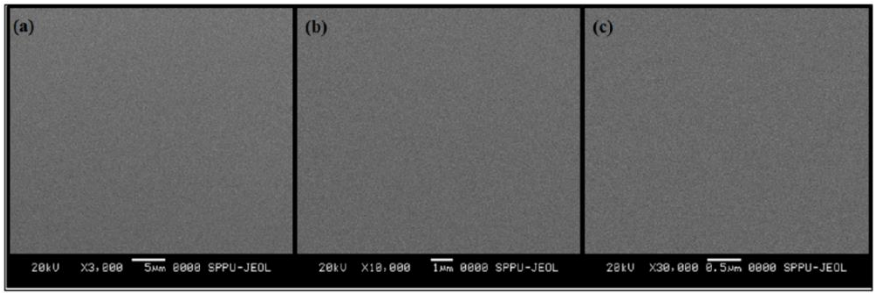

Fig. 3. SEM images of sample SHE-I at (a) 3000, (b) 10000, and (c) 30000 X magnifications.

3.2.3. *X-Ray diffraction analysis (XRD)*

The XRD patterns of sample SHE-I, copolymer poly (AAm-co-VI), and polysaccharide CMC are shown in Figs. 4a-c, respectively. It may be noticed in Fig. 4c that the XRD pattern contains a sharp peak at 2θ value of 20.43 degrees, thus suggesting the crystalline nature of the polymer CMC. This may probably be attributed to the presence of galactose units that form a crystalline region due to the H-bonded arrangement. In addition, a small shoulder between 35° and 45° suggests some amorphous nature also [26]. The XRD pattern of poly (AAm-co-VI), as shown in Fig. 4b, also shows a relatively wider peak at 23.41 degrees, probably due to the polymer network [27]. It is also noteworthy that two sharp but low-intensity peaks at 29.42 and 31.62° are also present in the diffraction pattern. This may probably be due to H-bonding interactions between amide and imidazole groups, thus forming a crystalline region. Finally, the XRD pattern of sample SHE-I, shown in Fig. 4c, almost contains the characteristic peaks of the above two polymers but with reduced intensity.

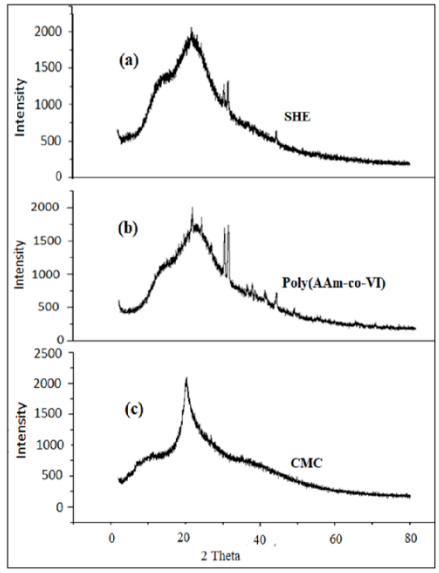

Fig. 4. XRD patterns of (a) CMC, (b) Poly(AAm-co-VI), and (c) sample SHE-I.

3.2.3. *Thermal gravimetric analysis (TGA)*

The thermal stability of the sample SHE-I was investigated, taking native CMC and poly(AAm-co-VI) as reference materials. Figs. 5a-c show TGA profiles of these materials, respectively. The TGA of native CMC exhibits a two-stage decomposition: Firstly, a weight loss of around 20 % is observed up to 200 °C, probably due to loss of moisture, and then a further weight loss of 40 % is observed up to 600 °C, which is attributable to the de-carboxylation and pyrolysis of polymeric backbone [28]. However, the TGA profiles of copolymer poly (AAm-co-VI) and SHE indicate that they are more stable than the native CMC. Their initial weight loss, due to moisture loss, is also comparatively small. The enhanced stability of SHE and copolymer poly(AAm-co-VI) is attributable to the presence of covalently bonded networks within the polymer matrix and hydrogen bonding interactions.

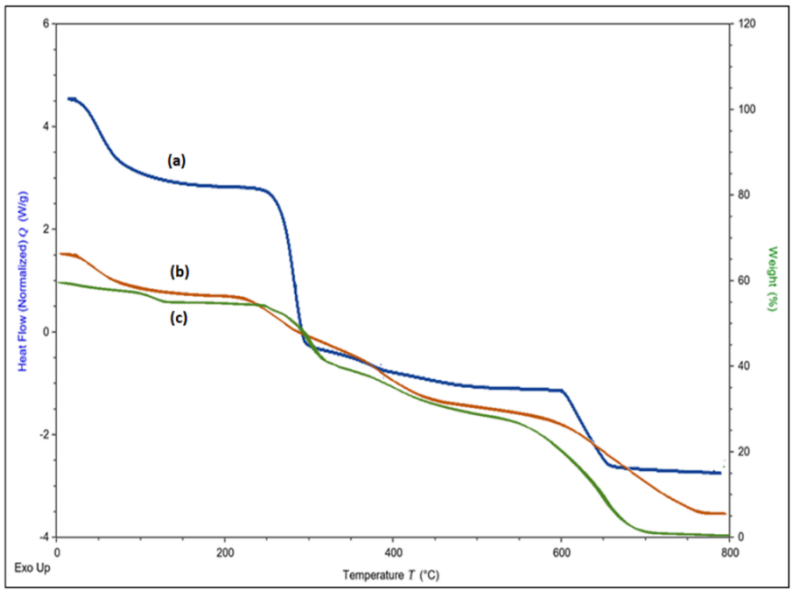

Fig. 5. TGA profiles of (a) CMC, (b) Poly(AAm-co-VI), and (c) sample SHE-I.

3.3. *Water absorption studies*

Results of water absorption kinetics of the sample SHE-I, in the media of pH 1.0, 6.8 (distilled water), and pH 7.4, are shown in Fig. 6a. It can be seen that the sample SHE-I demonstrates a fast swelling in pH 1.0, while the kinetic water uptake profiles of the sample in distilled water and in the medium of pH 7.4 run almost coinciding with each other. The higher water uptake in the swelling medium of pH 1.0 may probably be attributed to the protonation of imidazole groups of VI, which is a component of the copolymer. As a result of de-protonation, the positively charged imidazole groups repel each other, thus unfolding

the polymer chains and letting more and more water enter the network. It was also observed that the hydrogel possessed fair shape stability in spite of the fact that no crosslinking agent was used in the preparation of SHE. It appears that in the pH 1.0 medium, carboxymethyl groups and –OH groups, present in CMC macromolecular chains, may produce intra-molecular H-bonding interactions. In addition, the intermolecular H-bonding interactions between amide groups of AAm and hydroxyl and carboxymethyl groups of CMC are also operative. The percent equilibrium swelling (PES) in the medium of pH 1.0 was 5170 (i.e., almost 52 times the initial weight). The SHE with such a high water content became very soft and slippery. However, still, it maintained its structural integrity. The dynamic water uptake profiles of the sample in the distilled water and in the medium pH 7.4 almost overlapped. The relatively lower uptake could be attributed to the absence of protonated /ionized groups within the polymer matrix. This prevented the polymer chains from unfolding and, therefore, allowed limited water invasion within the SHE network. The kinetic water uptake data was interpreted in terms of well-known 'Power functions and 'Schott models (equations not shown). The linear plots, shown in Figs. 6(b)-(c), respectively, were used to calculate respective kinetic parameters. All the parameters are given in Table 2. A close look at Table 2 reveals that a high degree of regression is obtained for the Power function model, thus indicating its fair suitability. On the other hand, the Schott model showed poor regressions, and the experimental and theoretical values of 'Percent Equilibrium Swelling' also did not match. It is also noteworthy that swelling exponent 'n,' obtained in the Power Function Model for the kinetic water uptake data in the medium of pH 1.0, is 0.738, thus indicating the chain relaxation behavior of the hydrogel.

The pH-dependent swelling behavior of the sample SHE-I was studied by observing variation in 'Percent Equilibrium Swelling' (PES) with the pH of the swelling media, in the range of 1.0 to 13. The results, as shown in Fig. 6(d), reveal that a 'U' shaped profile is obtained, indicating a higher PES in the media of pH 1.0 (i.e., 5170) as well as in pH 13.0 (i.e., 5163). The highest water uptake in the pH 1.0 and 13.0 media may be explained as follows: In pH 1.0, the imidazole groups get protonated, and the unfolding of chains occurs. This allows a huge quantity of water molecules to enter into the network. On the other hand, when the pH of the swelling medium is 13.0, the highly alkaline medium induces hydrolysis of amide groups of constituents AAm of copolymer poly (AAm-co-VI) into carboxylic groups, which get ionized to yield negatively charged $–COO^-$ groups along the copolymeric chains.

Hence, as a result of electrostatic repulsion, chains are unfolded and allow more and more water molecules to enter. In addition, ionized carboxymethyl groups also contribute to this unfolding. However, in the vicinity of neutral pH, i.e., 7.0, the polymer chains of CMC and poly (AAm-co-VI) are entangled with each other, thus providing a folded network with H-bonding interactions, which act as additional physical crosslinks. Therefore, water absorption is restricted in this case. Finally, the PSE was 5163 in a pH medium of 13.0 was attributable to the fact that in the strong alkaline medium, the acrylamide molecules, present within the copolymer chains, were hydrolyzed to yield –COOH groups which, subsequently, were ionized to yield negatively charged carboxylate

ions along the copolymeric chains and thus, induced chain relaxation process within the polymer matrix. This resulted in higher water uptake.

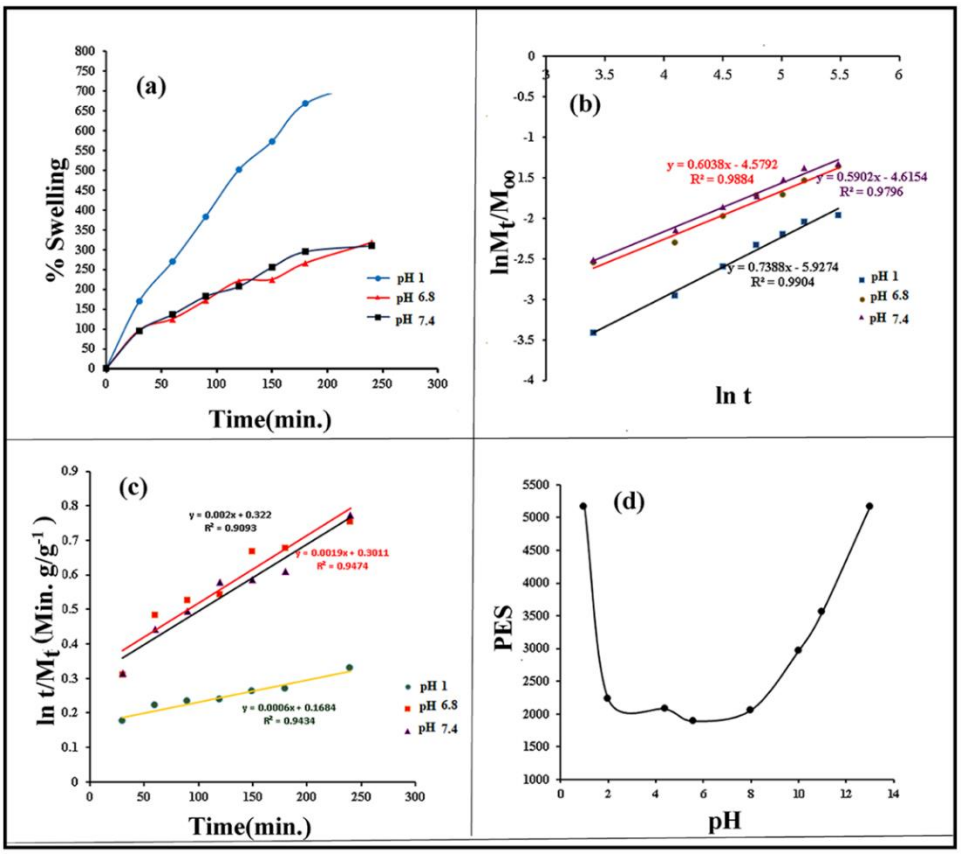

Fig. 6. (a) Dynamic water uptake profile of sample SHE-I, (b) Power function, (c) Schott models for water uptake data, and (d) pH-dependent equilibrium water uptake of sample SHE-I.

Table 2. Parameters associated with kinetic models were used to interpret the water uptake data for sample SHE-I at room temperature.

pH of the medium	Kinetic models						
	Power function model			Schott model			
	k x 10^3	n	R^2	k_2 x10^6	$M_{\infty(th.)}$ (%)	$M_{\infty(exp.)}$ (%)	R^2
1.0	2.7	0.7388	0.9904	2.13	1666.6	5170.6	0.9434
6.8	9.9	0.5902	0.9796	12.42	500.5	1237.8	0.9093
7.4	10.3	0.6038	0.9884	11.98	526.2	1165.8	0.9474

3.4. *Self-healing behavior*

As mentioned earlier, the presence of H-bonding interactions in a polymer matrix renders self-healing properties to it. In this work, the self-healing behavior of the sample in the 'LED" experiment confirmed SHE-I. As can be seen in Fig. 7a, initially, the intact SHE

works as a connecting medium and allows the electric current to flow through, and hence the LED bulb glows. However, when the SHE is cut into two pieces, the circuit is broken, and therefore the LED blows off (Fig. 7b). Finally, when the two cut ends are brought into contact for five minutes, the hydrogel is self-healed, and the continuity is again restored. This again maintains the flow of electricity, thus finally allowing the LED bulb to glow (Fig. 7c). These results may be explained as follows: when the hydrogel is cut into two pieces, the H-bonding interactions are ruptured, and the current supply is stopped. However, when the two ends are brought into contact, the imidazole, hydroxyl, and amide groups, present along the surfaces of the two cut ends, bind with each other again, thus making a continuous path for the flow of electric current. The re-formation of H-bonds across the interface of the terminals of cut ends is the major reason for the self-healing of hydrogel electrolytes.

In order to confirm whether the healed SHE also exhibited the same strength as the original one, a piece of hydrogel with a length of 7 cm was stretched at its two ends. The percent elongation was almost 200 %, as shown in Figs. 7d-e. Now, the strip was cut into two pieces, and the cut ends were brought into contact to start the healing process (Fig. 7f). After the gel was healed properly, the strip was again stretched at both ends (Fig. 7g). It was observed that the strip was elongated to 157 %, thus indicating that the strength of the hydrogel strip was restored to a great extent after healing through H-bonding interactions. The self-healing property of SHE was further demonstrated by cutting a long piece of hydrogel into small pieces and then joining them to make some geometries, as shown in Fig. 7h. It is also worth mentioning here that the geometries made had proper strength, and they could not be deformed by external stress.

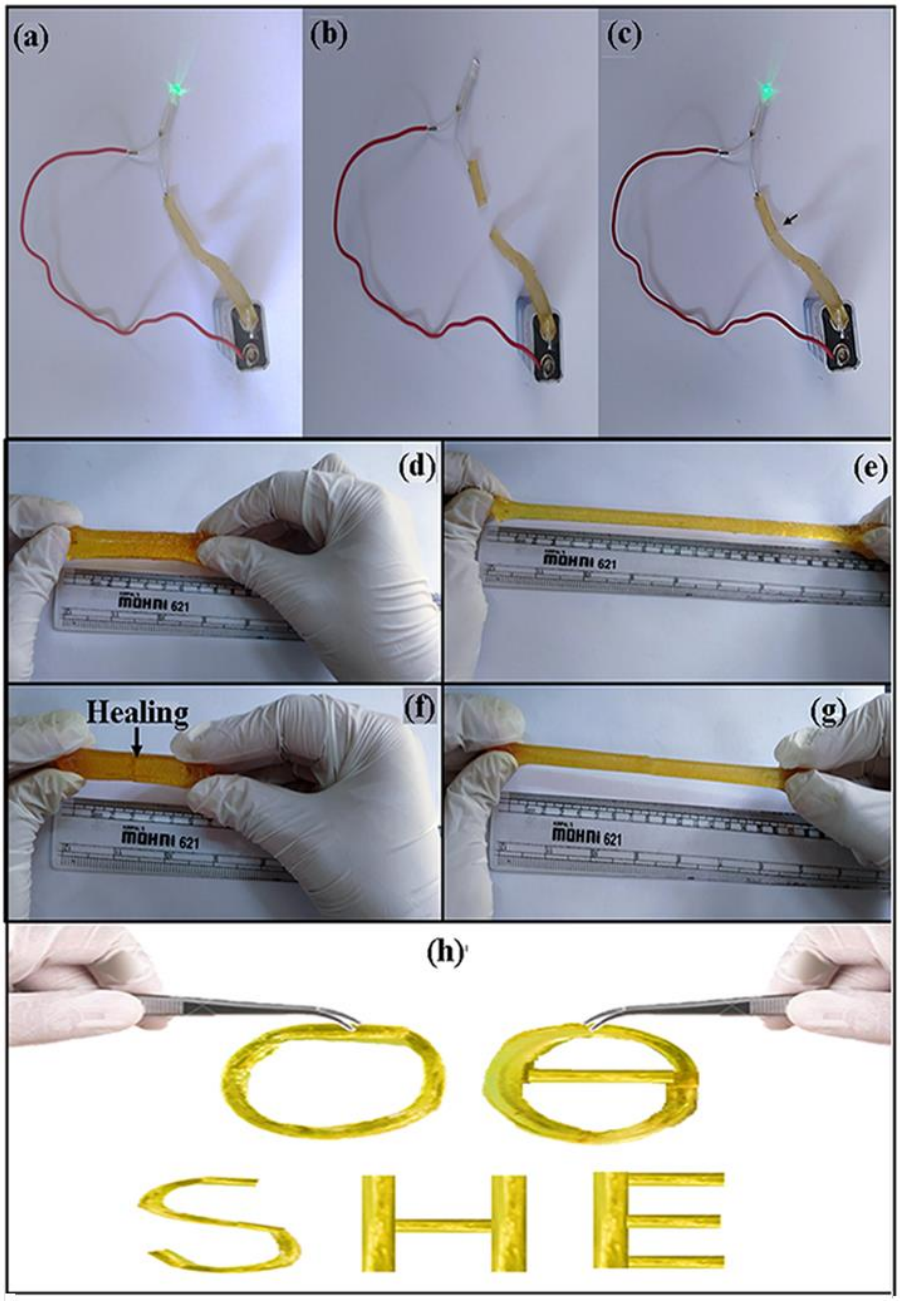

Fig. 7. (a) SHE acts as a conductor and glows the LED bulb, (b) the gel is cut and the LED blows off, (c) LED glows again when two cut ends put together and gel is healed, (d) and (e) a 7 cm gel piece elongates to 200 %, (f) gel is cut into two pieces and allowed to heal, (g) healed gel showing elongation of 157 % and (h) some geometries fabricated using pieces of hydrogel.

4. Conclusion

From the above study, it may be concluded that hydrogel SHE, composed of CMC and poly(AAm-co-VI), exhibits excellent self-healing properties. This was confirmed by the "LED bulb glow" experiment. Moreover, the hydrogel regained almost 80 % of its mechanical strength after self-healing. The hydrogel swelled to around 5170 and 5163 percent in the pH 1.0 and 13.0 media, respectively. The water absorption dynamics were best interpreted in terms of the 'power function model.' Indeed, these self-healing hydrogels have a wide range of applications in different fields like wearable, flexible devices, electronic skin, biomedicine, tissue engineering, cell therapy, wound dressing, etc.

Acknowledgment

The authors are thankful to S. Tiwari for providing instrumental facilities for analysis.

References

1. Z. Chen, J. Liu, Y. Chen, X. Zheng, H. Liu, and H. Li, ACS Appl. Mater. Interfaces **13**, 1353 (2020). https://doi.org/10.1021/acsami.0c16719
2. M. Hina, S. Bashir, K. Kamran, J. Iqbal, S. Ramesh, and K. Ramesh, Mater. Chem. Phys. **273**, 125 (2021). https://doi.org/10.1016/j.matchemphys.2021.125125
3. S. Li, X. Zhou, Y. Dong, and Li, J. Macromol. Rapid Communi. **41**, 2000444 (2020). https://doi.org/10.1002/marc.202070009
4. S. Li, Y. Cong, and J. Fu, J. Mater. Chem. B **9**, 4423 (2021). https://doi.org/10.1039/D1TB00523E
5. Y. Wang, M. Zhu, X. Wei, J. Yu, Z. Li, and B. Ding, Chem. Eng. J. **425**, ID 130599 (2021). https://doi.org/10.1016/j.cej.2021.130599
6. H. Liu, T. Chen, C. Dong, and X. Pan, Hydrogels **27**, 4647 (2020). https://doi.org/10.2174/0929867327666200408115817
7. E. Ahmadian, S. M. Dizaj, A. Eftekhari, E. Dalir, P. Vahedi et al., Drug Res. **70**, 6 (2019). https://doi.org/10.1055/a-0991-7585
8. G. Chen, W. Tang, X. Wang, X. Zhao, C. Chen, and Z. Zhu, Polymers **11**, ID 1420 (2019). https://doi.org/10.3390/polym11091420
9. H. Hong, Y. B. Seo, D. Y. Kim, J. S. Lee, Y. J. Lee et al., Biomaterials **232**, ID 119679 (2020). https://doi.org/10.1016/j.biomaterials.2019.119679
10. M. Askari, M. A. Naniz, M. Kouhi, A. Saberi, A. Zolfagharian, and M. Bodaghi, Biomater. Sci. **9**, 535 (2021). https://doi.org/10.1039/D0BM00973C
11. H. Pangli, S. Vatanpour, S. Hortamani, R. Jalili, and A. Ghahary, J. Burn Care Res. **42**, 785 (2020). https://doi.org/10.1093/jbcr/iraa205
12. J. Amirian, Y. Zeng, M. I. Shekh, G. Sharma, F. J. Stadler et al., Carbohydr. Polym. **251**, ID 117005 (2020). https://doi.org/10.1016/j.carbpol.2020.117005
13. S. Qiang, D. Lijie, Z. Meifang, C. Xuetong, and G. G. Hui, Mater. Chem. Phys. **193**, 57 (2017). https://doi.org/10.1016/j.matchemphys.2017.02.018
14. S. Y. Lee, S. I. Jeon, S. B. Sim, Byun, and C.-H. Ahn, Acta Biomaterialia **131**, 286 (2021). https://doi.org/10.1016/j.actbio.2021.07.004
15. F. Chen, Y. He, Z. Li, B. Q. Xu, X. Ye, and Y. Li, Int. J. Pharm. **606,** ID 120938 (2021). https://doi.org/10.1016/j.ijpharm.2021.120938
16. Y. Li, C. Liu, X. Lv, and S. Sun, Soft Matter **17**, 2142 (2020). https://doi.org/10.1039/D0SM01998D

17. L. Debertrand, J. Zhao, C. Creton, and T. Narita, Gels **7**, ID 72 (2021). https://doi.org/10.3390/gels7020072
18. L. Hammer, N. J. Van Zee, and R. Nicolaÿ, Polymers **13**, ID 396 (2021). https://doi.org/10.3390/polym13030396
19. F. Ding, Y Zou, S. Wu, and X. Zou, Polymer **206**, ID 122907 (2020). https://doi.org/10.1016/j.polymer.2020.122907
20. Y. -J. Wan, K. Rajavel, X. -M. Li, X. -Y. Wang et al., Chem. Eng. J. **408**, ID 127303 (2020). https://doi.org/10.1016/j.cej.2021.129962
21. A. E. Hoshoudy, S. Desouky, A. Al-sabagh, M. El-kady, and M. Betiha, Int. J. Oil **3**, 47 (2015). https://doi.org/10.1155/2015/318708
22. A. Kara, L. Uzun, N. Beşirli, and A. Denizli, J. Hazard. Mater. **106**, 93 (2004).
23. S. M. Abdellatif Soliman, M. F. Sanad, and A. E. Shalan, RSC Adv. **11**, 11541 (2021). https://doi.org/10.1039/D1RA01874D
24. Z. Ajji and A. M. Ali, J. Hazard. Mater. **173**, 71 (2010). https://doi.org/10.1016/j.jhazmat.2009.08.049
25. Z. Ahmad and M. I. N. Isa, Adv. Mater. Res. **1107**, 223 (2015). https://doi.org/10.4028/b-QYcQb3
26. K. H. Kamarudin and M. I. N. Isa, Int. J. Phys. Sci. **8,** 1581 (2013). https://doi.org/10.5897/IJPS2013.3962
27. K. Varaprasad, Y. M. Mohan, S. Ravindra, N. N. Reddy, K. Vimala et al., J. Appl. Polym. Sci. **115**, 1199 (2010). https://doi.org/10.1002/app.31249
28. A. Pettignano, A. Charlot, and E. Fleury, Polymers **11**, ID 1227 (2019). https://doi.org/10.3390/polym11071227